II International Conference on Particle-based Methods – Fundamentals and Applications
PARTICLES 2011
E. Oñate and D.R.J. Owen (Eds)

SMOOTHED PARTICLE HYDRODYNAMICS MODELING OF HYDRAULIC JUMPS

PATRICK JONSSON[*], PÄR JONSÉN[†], PATRIK ANDREASSON[*], T. STAFFAN LUNDSTRÖM[*] AND J. GUNNAR I. HELLSTRÖM[*]

[*] Division of Fluid and Experimental Mechanics
Luleå University of Technology (LTU)
SE-971 87, Luleå, Sweden
e-mail: patrick.jonsson@ltu.se, www.ltu.se

[†] Division of Mechanics of Solid Materials
Luleå University of Technology (LTU)
SE-971 87, Luleå, Sweden
e-mail: par.jonsen@ltu.se, www.ltu.se

Key words: hydraulic jump, smoothed particle hydrodynamics, sph, particle study.

Abstract. This study focus on Smoothed Particle Hydrodynamics (SPH) modeling of two-dimensional hydraulic jumps in horizontal open channel flows. Insights to the complex dynamics of hydraulic jumps in a generalized test case serves as a knowledgebase for real world applications such as spillway channel flows in hydropower systems. In spillways, the strong energy dissipative mechanism associated with hydraulic jumps is a utilized feature to reduce negative effects of erosion to spillway channel banks and in the old river bed.

The SPH-method with its mesh-free Lagrangian formulation and adaptive nature results in a method that handles extremely large deformations and numerous publications using the SPH-method for free-surface flow computations can be found in the literature.

Hence, the main objectives with this work are to explore the SPH-methods capabilities to accurately capture the main features of a hydraulic jump and to investigate the influence of the number of particles that represent the system.

The geometrical setup consists of an inlet which discharges to a horizontal plane with an attached weir close to the outlet. To investigate the influence of the number of particles that represents the system, three initial interparticle distances were studied, coarse, mid and fine.

For all cases it is shown that the SPH-method accurately captures the main features of a hydraulic jump such as the transition between supercritical- and subcritical flow and the dynamics of the highly turbulent roller and the air entrapment process. The latter was captured even though a single phase was modeled only. Comparison of theoretically derived values and numerical results show good agreement for the coarse and mid cases. However, the fine case show oscillating tendencies which might be due to inherent numerical instabilities of the SPH-method or it might show a more physically correct solution. Further validation with experimental results is needed to clarify these issues.

1 INTRODUCTION

The main components of a large scale hydropower station are a large reservoir dam where rain and melt water is stored and the turbine/generator assembly which converts the potential energy stored in the water into electricity[1]. The hydropower sector contributes to almost half of the total power production in Sweden[2]. However, the overall contribution from the hydropower sector varies throughout the year due to variation in energy demand from the consumers which in turn is due to seasonal variation in temperature and maintenance shutdown of industrial processes. As production varies throughout the year and the amount of precipitation is uncontrollable the need to find ways to handle the water head in the reservoir is crucial to obtain optimal working conditions. If the inherent flow regulation by generation is insufficient, spillways are engaged. When spillways are used the potential energy of the water is converted to kinetic energy potentially causing erosion problems to structures in the spillway channel as well as in other water-ways downstream the spillway like old river beds. An effective way to reduce the high kinetic energy levels is to design the spillway channels to trigger a hydraulic jump which is a natural occurring phenomenon in free flowing fluids characterized by large energy dissipation mechanisms[3]. The main feature of a hydraulic jump is a sudden transition of shallow and fast moving flow into a relatively slow moving flow with rise of the fluid surface to keep continuity. The transition phase is known as the roller where the free surface is highly disturbed and air entrapment occurs.

Modeling of highly disturbed free surface flows such as the hydraulic jump is complex when grid based method is used. Severe problems with mesh entanglement and determination of the free surface have been encountered[4]. Meshfree methods such as the Smooth Particle Hydrodynamic (SPH) method have been shown to be a good alternative to grid based methods to overcome the above stated problems[5,6]. The SPH-method has matured rapidly during the last decade or even years and was thus chosen as the computational method.

The aim with this work is thus to explore the capability of the SPH-methods to accurately capture the main features of a hydraulic jump and to investigate the influence of the number of particles that represent the system.

2 METHOD

2.1 Smoothed particle hydrodynamics

Smoothed Particle Hydrodynamics (SPH) is a meshfree, adaptive, Lagrangian particle method for modeling fluid flow. The technique was first invented independently by Lucy[7] and Gingold and Monaghan[8] in the late seventies to solve astrophysical problems in three-dimensional open space. Movement of astronomical particles resembles the motion of fluids, thus it can be modeled by the governing equations of classical Newtonian hydrodynamics. The method did not attract much consideration in the research community until the beginning of the 1990 when the method was successfully applied to other areas than astrophysics. Today, the SPH-method has matured even further and is applied in a wide range of fields such as solid mechanics (e.g. high velocity impact and granular flow problems) and fluid dynamics (e.g. free-surface flows, incompressible and compressible flows).

In the SPH-method, the fluid domain is represented by a set of non-connected particles which possess individual material properties such as mass, density, velocity, position and

pressure[9]. Besides representing the problem domain and acting as information carriers the particles also act as the computational frame for the field function approximations. As the particles move with the fluid the material properties changes over time due to interaction with neighboring particles, hence making the technique a pure adaptive, mesh-free Lagrangian method. With adaptive is meant that at each time step the field approximation is done based on the local distribution of neighboring particles. The adaptive nature of the SPH-method together with the non-connectivity between the particles results in a method that is able to handle very large deformations as is the case for highly disordered free-surface flows such as hydraulic jumps.

To further clarify the methodology of the SPH-method, the following key steps is employed to reduce the partial differential equation (PDEs) governing the problem at hand to a set of ordinary differential equations (ODEs).

1. The problem domain is represented by a set of non-connected particles.
2. The *integral representation method* is used for field function approximation, known as the *kernel approximation*.
3. The kernel approximation is then further approximated using particles, i.e. the *particle approximation*. The particle approximation replaces the integral in the kernel approximation by summations over all neighboring particles in the so called *support domain*.
4. The summations or the particle approximation are performed at each time step, hence the adaptive nature of the SPH-method as particle position and the magnitude of the individual properties varies with time.
5. The particle approximation is employed to all terms of the field functions and reduces the PDEs to discretized ODEs with respect to time only.
6. The ODEs are solved using standard explicit integration algorithms.

A more detailed description of the methodology and the *kernel-* and *particle approximations* can be found in the textbook by Liu and Liu[9].

As concluded in previous work[10,11] the SPH-method do not necessarily behave in the same manner as mesh-based computational methods where refinement of the mesh is anticipated to yield better solutions of the PDEs. Instead, further refinement or more particles in the SPH-method might lead to deterioration of solutions or even divergent behaviour. This may be caused by inherent numerical instabilities of the SPH-method.

2.2 Hydraulic jump

The main characteristic of a hydraulic jump is the sudden transition of rapid shallow flow to slow moving flow with rise of the fluid surface also known as a transition from supercritical to subcritical flow[3]. The transition is strongly dissipative which is favourable when energy should be consumed as when kinetic energy levels should be reduced in spillway flows. Further characteristics of hydraulic jumps is the development of a large-scale highly turbulent zone known as the “roller” with surface waves and spray, energy dissipation and air entrapment.

As stated above the hydraulic jump is characterized by a supercritical and a subcritical region where the depths are significantly different. These depths d_1 and d_2 are referred to as *conjugate depths* and can be seen in the schematic Figure 1.

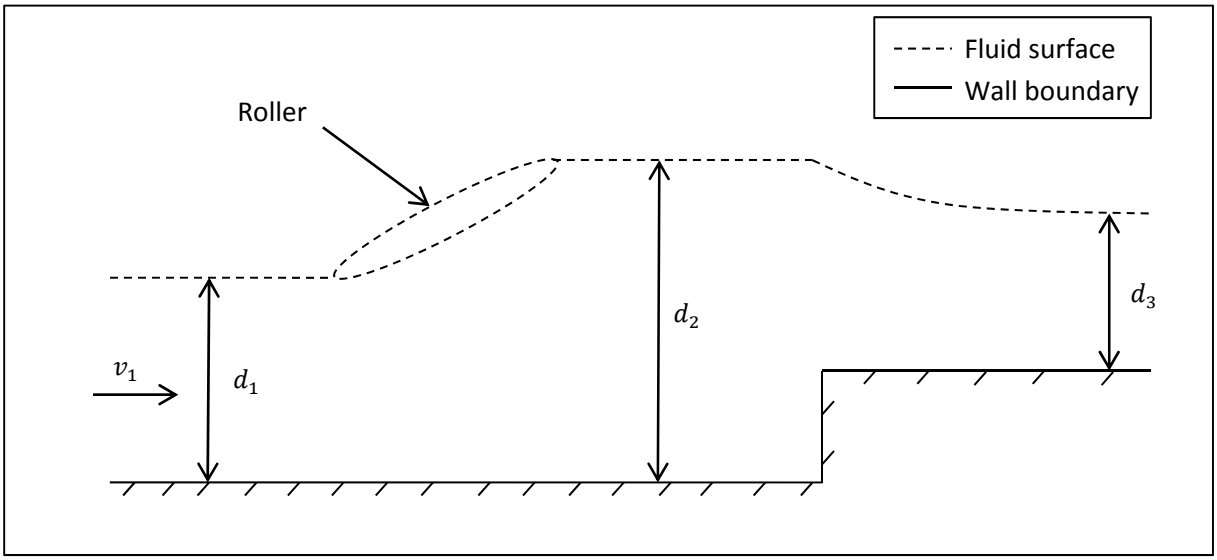

Figure 1: Schematic figure of the hydraulic jump showing the conjugate depths d_1 and d_2 and the depth d_3 past the weir.

A dimensionless relation between the conjugate depths can easily be derived from continuity, momentum and energy equations for a rectangular channel by assuming hydrostatic pressure distribution and uniform velocity distribution at the up- and downstream end of the control volume. Furthermore, the friction between the bottom and the fluid and the slope of the bottom is both assumed to be zero. With these assumptions the conservations equations yield the dimensionless relation between the conjugate depths for a rectangular channel as,

$$\frac{d_2}{d_1} = \frac{1}{2}\left(\sqrt{1 + 8Fr_1^2} - 1\right) \tag{1}$$

where Fr_1 is the upstream Froude number,

$$Fr_1 = \frac{v_1}{\sqrt{g d_1}} \tag{2}$$

which by definition must be greater than one. The upstream Froude number is also used as an indicator of the general characteristics of the jump in a rectangular horizontal channel as different upstream Froude numbers produce different types of hydraulic jumps[3].

Furthermore, the depth d_3 is derived in a similar manner with the same assumptions as above, further details can be found in the textbook by Chanson[3].

2.3 Numerical setup

To reduce the complexity of modeling a three dimensional spillway channel with adherent hydraulic jump a two dimensional, horizontal and single phase (water) model is studied here. Following previous work[12,13] the material model MAT_NULL is used to model water with density $\rho = 1000\ kg/m^3$ and dynamic viscosity $\mu = 0.0015\ Pa\ s$. The null material has no shear stiffness or yield strength and behaves in a fluid-like manner[14]. As the dynamic viscosity μ is nonzero, a deviatoric viscous stress of the form,

$$\sigma'_{ij} = \mu\dot{\varepsilon}'_{ij} \tag{3}$$

is computed where $\dot{\varepsilon}'_{ij}$ is the deviatoric strain rate[15]. Furthermore, the null material must also be used together with an equation of state (EOS) defining the pressure in the material. Varas et al.[13] used the Gruneisen equation of state which employs the cubic shock velocity-particle velocity, which also was used in this work. The wall boundaries were modeled as rigid shell finite elements and the interaction between the boundaries and the SPH-particles was governed by a penalty based node to surface contact-algorithm.

The geometrical setup of the problem can be seen in Figure 2 where the fluid enters the domain using the BOUNDARY_SPH_FLOW inlet condition with an prescribed inlet velocity of $v_1 = 1.5\ m/s$ and depth $d_1 = 0.02\ m$. The horizontal plane situated between the inlet and the weir measures $1.1\ m$ and is prefilled to a depth equal to weir height, i.e. d_1. Both the prefill of the horizontal plane and the weir assembly was introduced to trigger the hydraulic jump faster. Furthermore, at $1.9\ m$ downstream of the inlet the outlet is situated.

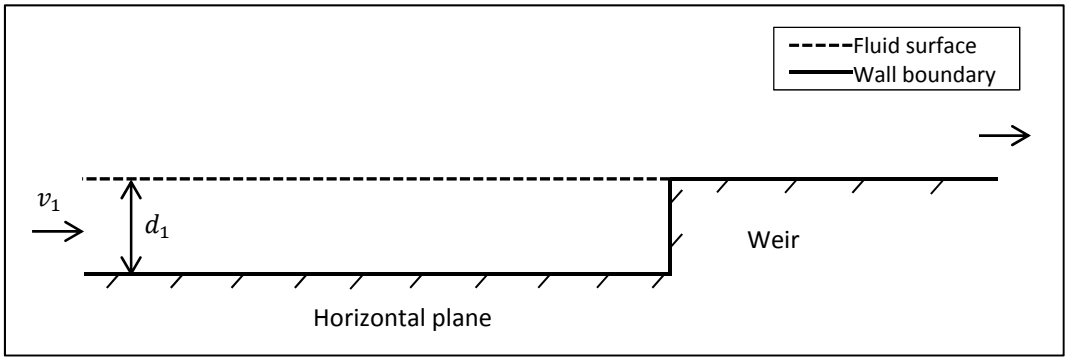

Figure 2: Geometrical setup at $t = 0\ s$.

Initial results indicated that after an initial transient phase of roughly $3.0\ s$ the hydraulic jump was fully developed. However, the roller region was non-stationary even after the initial transient phase and traveled upstream toward the gate with very low velocity, hence all subsequent simulation were run for five seconds to include such phenomena. Three different initial interparticle spacing Δl ($\Delta l = \Delta x = \Delta y$) of $0.005\ m$ $(coarse)$, $0.004\ m$ (mid), and $0.002\ m$ $(fine)$ were used to investigate the influence of the number of particles that represent the system. The total number of particles and the overall computational time for each case is summarized in Table 1.

Table 1: The total number of particles and the overall computational time for each case.

Case	Total number of particles	Computational time $[h]$
$Coarse\ (\Delta l = 0.005m)$	6880	19 (12 $cores$)
$Mid\ (\Delta l = 0.004m)$	10750	29 (8 $cores$)
$Fine\ (\Delta l = 0.002m)$	43000	186 (12 $cores$)

All simulations where done using the commercial available software package LSTC LS-DYNA v. 971 R5.1.1 on HP Z600 Linux machines with eight to twelve cores.

3 RESULTS AND DISCUSSION

This part will start with a qualitative comparison of the three cases at successive time steps and end with a quantitative comparison of theoretically derived values and results from the simulations.

At $t = 0.0\ s$ the fast incoming fluid begins to flow into the initially stationary fluid which starts to move together downstream, i.e. in the positive x-direction. A wave forms and breaks as more water flows onto the horizontal plane and at roughly $1.0\ s$ it reaches the weir and starts to spill over. The fluid reaches the outlet at roughly $1.5\ s$ and in the meantime the roller region has moved closer to the weir. The roller continues to move downstream towards the weir until roughly $3.0\ s$ when the velocity of the roller declines rapidly and change direction. Past $3.0\ s$ a quasi-stationary state is attained as the velocity of roller upstream is very low. Figures 3-5 shows the three cases using the above stated number of particles with color coded velocities in the positive x-direction.

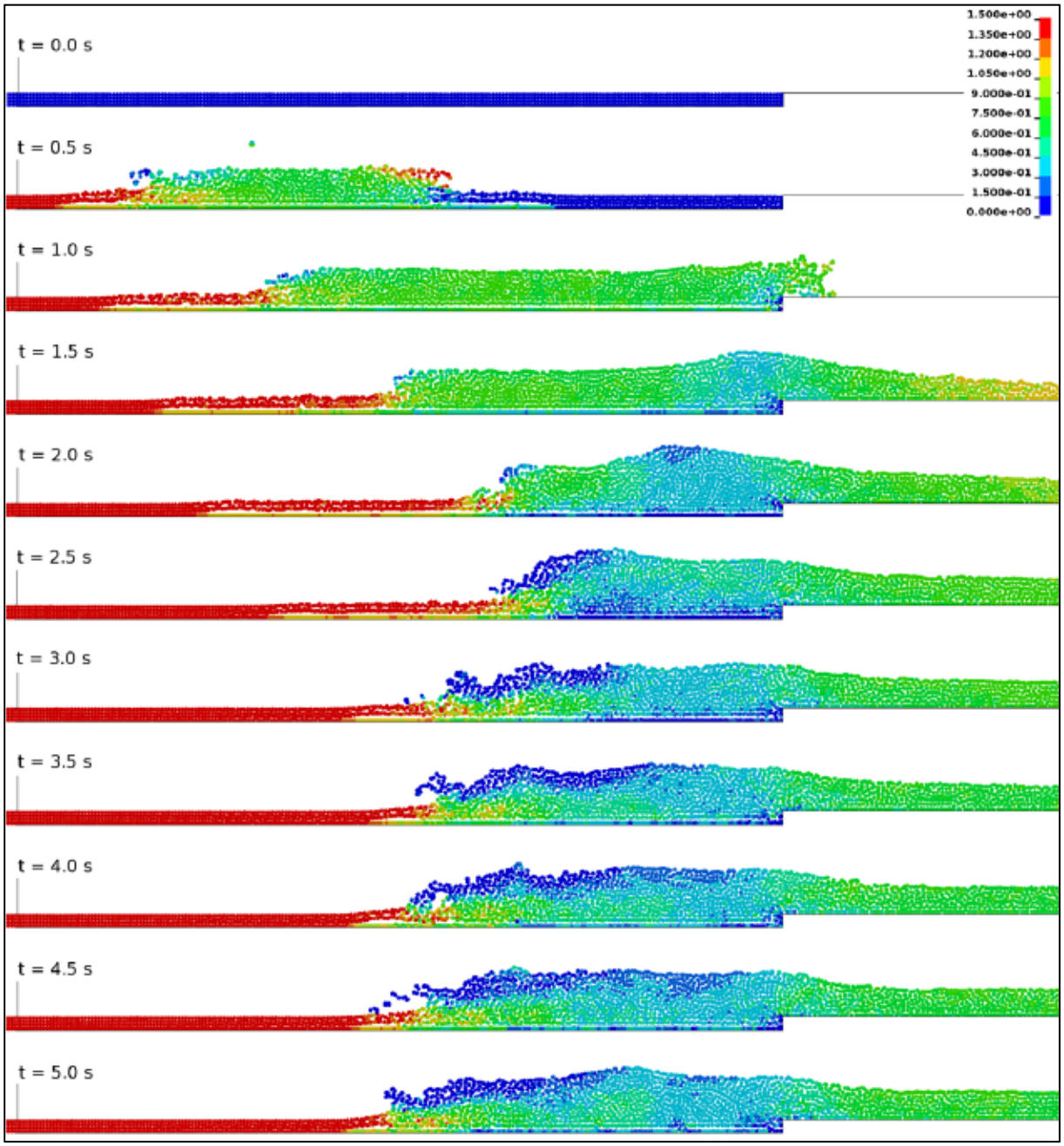

Figure 3: Visualization of the coarse ($\Delta l = 0.005\ m$) case at successive time steps with color coded velocities in the positive x-direction.

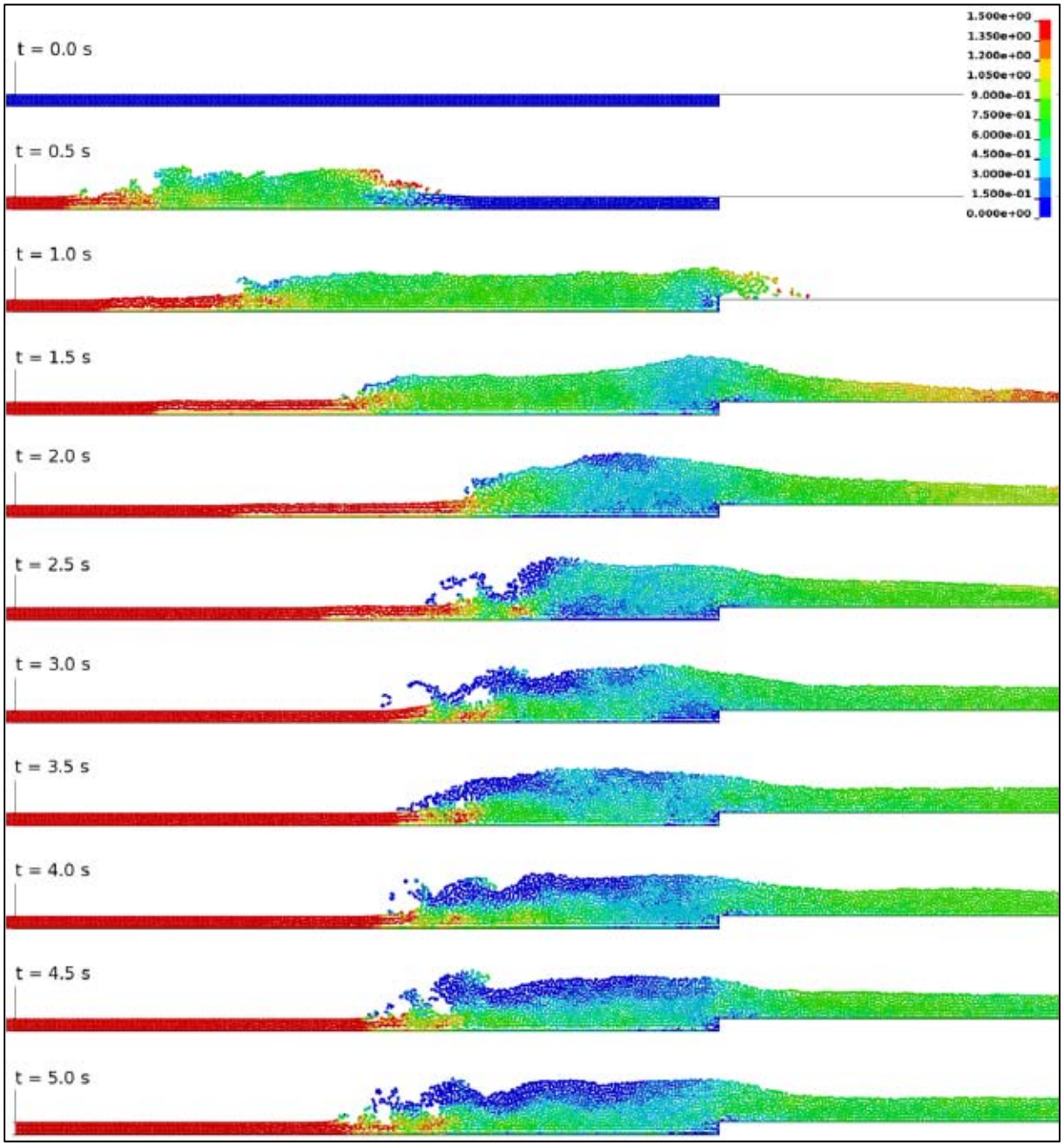

Figure 4: Visualization of the mid ($\Delta l = 0.004\ m$) case at successive time steps with color coded velocities in the positive x-direction.

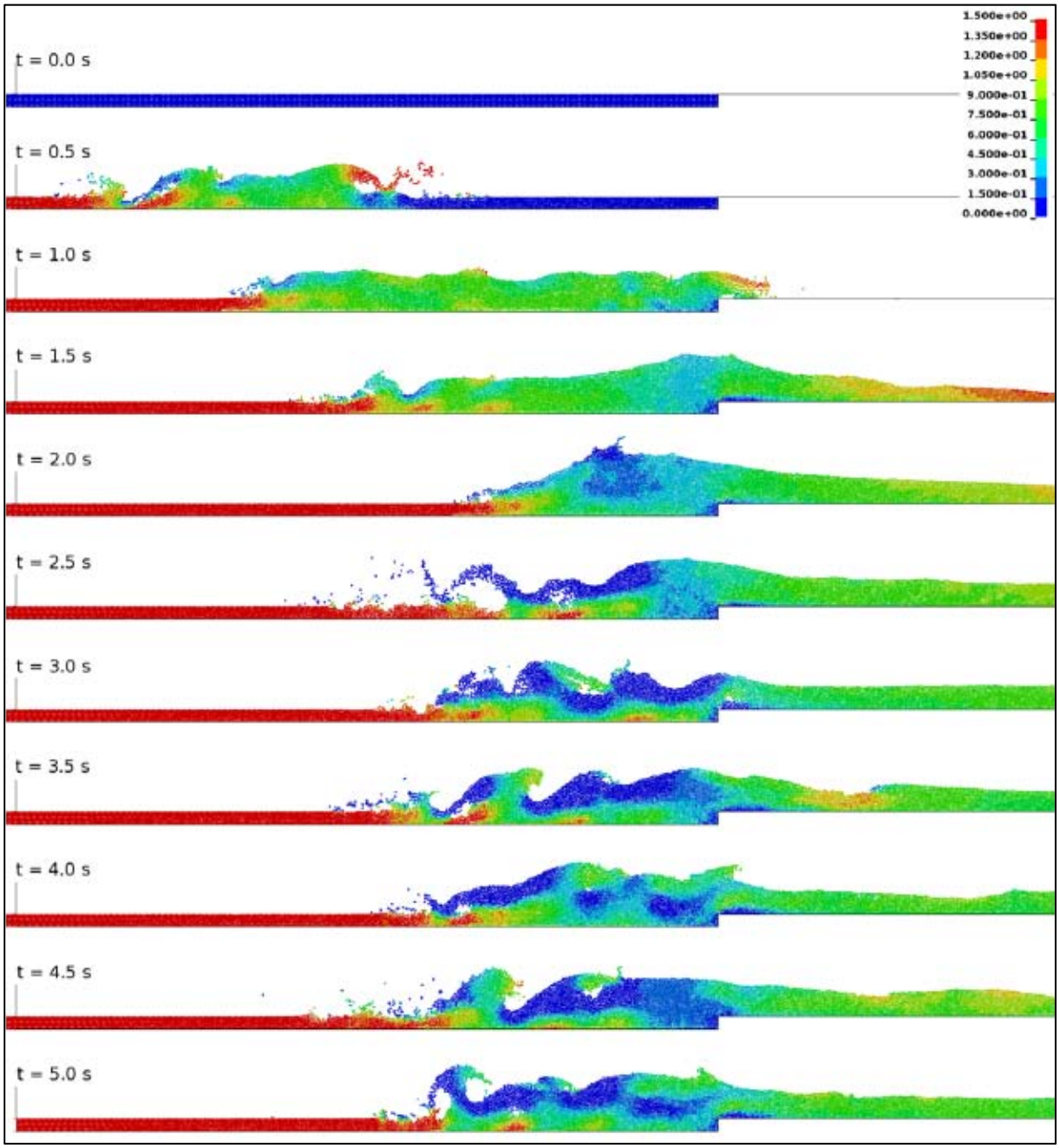

Figure 5: Visualization of the fine ($\Delta l = 0.002\ m$) case at successive time steps with color coded velocities in the positive x-direction.

Comparing the results in Figures 3-5 in a qualitative manner both the coarser cases produces smooth hydraulic jumps with well-defined free-surfaces especially past the roller region. The fine case behaves in a more chaotic manner with large oscillation of the free-surface which is clearly seen in the subcritical region past the roller. However, all three cases capture the main features of a hydraulic jump such as the high velocity small depth supercritical- and low velocity large depth subcritical region. Furthermore, the highly

turbulent roller where air entrapment occurs is clearly visible in all cases even though a single phase has been modeled only.

As stated above, the hydraulic jump is fully developed at roughly 3.0 s hence all data from the simulations was obtained past this time at intervals of 0.5 s. In this work, the depth d_2 in the subcritical section and the depth d_3 in the contraction past the weir have been evaluated only. However, as can be seen in Figures 3-5 the velocity field can be obtained as well as other quantities such as pressure distribution and acceleration of individual particles. To determine the position of the free-surface and hence the depths d_2 and d_3, the average value of the y-coordinate of particles located at the assumed free-surface with half the initial interparticle distance added was used. Particles in the interval of [1.0 1.1] and [1.5 1.6] in the x-direction was used to determine d_2 and d_3 respectively.

With the present inlet condition $v_1 = 1.5\ m/s$ and depth $d_1 = 0.02\ m$, $Fr = 3.4$ and consequently $d_2 = 0.086\ m$ and $d_3 = 0.058\ m$. Results obtained from the simulations of the depths d_2 and d_3 are summarized in Tables 2-3.

Table 2: The theoretically derived depth d_2 and numerical results obtained for the three cases coarse, mid and fine.

$\boldsymbol{time}\ [s]$	$\boldsymbol{d_{2,theory}}\ [m]$	$\boldsymbol{d_{2,c}}\ [m]$	$\boldsymbol{d_{2,m}}\ [m]$	$\boldsymbol{d_{2,f}}\ [m]$
3.0	0.086	0.083	0.087	0.067
3.5	0.086	0.082	0.082	0.088
4.0	0.086	0.083	0.083	0.083
4.5	0.086	0.084	0.083	0.082
5.0	0.086	0.081	0.086	0.088

Table 3: The theoretically derived depth d_3 and numerical results obtained for the three cases coarse, mid and fine.

$\boldsymbol{time}\ [s]$	$\boldsymbol{d_{3,theory}}\ [m]$	$\boldsymbol{d_{3,c}}\ [m]$	$\boldsymbol{d_{3,m}}\ [m]$	$\boldsymbol{d_{3,f}}\ [m]$
3.0	0.058	0.060	0.057	0.060
3.5	0.058	0.056	0.059	0.055
4.0	0.058	0.058	0.061	0.053
4.5	0.058	0.058	0.058	0.061
5.0	0.058	0.058	0.058	0.052

As derived from Tables 2-3 both the coarse and mid cases agrees well with the theoretically derived values of both depths. However, the depths for the fine case oscillates heavily compared to other two. This chaotic behavior might be due to inherent numerical instabilities of the SPH-method satisfying the conclusions of previous works[10,11]. However, it might be the most physically correct solution implying that the threshold of refinement when a divergent behavior is obtained is not reached or it might not be applicable to the current problem. Further validation through experiments is needed in order to confirm which of the above statements is correct. Experiments of current or similar geometrical setup can be found in the literature[16] hence such analysis has great potential for future work efforts.

As mentioned above, the pressure distribution is easily obtained from simulation data. However, as the pressure was greatly over predicted by the Gruneisen EOS no such figures is

shown. This behavior is at this stage not known to the authors but the validity of the Gruneisen EOS and the parameters used for current problem might be questionable.

5 CONCLUSIONS

The capabilities of the SPH-method to accurately capture the main features of a hydraulic jump such as the transition between supercritical- and subcritical flow has been demonstrated. Furthermore, the dynamics of the highly turbulent roller and the air entrapment process has been visualized even though a single phase has been modeled only. Comparison of theoretically derived values and numerical results of the depth d_2 in the subcritical section and the depth d_3 in the contraction past the weir show good agreement for the coarse and mid cases. The fine case show oscillating tendencies which might be due to inherent numerical instabilities of the SPH-method or it might show a more physically correct solution. Further validation through experiment is needed to clarify these issues.

6 ACKNOWLEDGEMENT

The research presented was carried out as a part of "Swedish Hydropower Centre - SVC". SVC has been established by the Swedish Energy Agency, Elforsk and Svenska Kraftnät together with Luleå University of Technology, The Royal Institute of Technology, Chalmers University of Technology and Uppsala University. www.svc.nu

REFERENCES

[1] Hellström, J. G. I. (2009). *Internal Erosion in Embankment Dams - Fluid Flow Through and Deformation of Porous Media.* Luleå: Luleå University of Technology.

[2] Sandberg, E. (2009, June 3). *Svensk energi*. Retrieved January 30, 2011, from http://www.svenskenergi.se/sv/Om-el/Elproduktion/

[3] Chanson, H. (2004). *The Hydraulics of Open Channel Flow: An Introduction.* Oxford: Elsevier Ltd.

[4] Scardovelli, R., & Zaleski, S. (1999). Direct numerical simulation of free-surface and interfacial flow. *Annual Review of Fluid Mechanics*, 567-603.

[5] López, D., Marivela, R., & Garrote, L. (2010). Smoothed particle hydrodynamics model applied to hydraulic structure: a hydraulic jump test case. *Journal of Hydraulic Research Vol. 48Extra Issue*, 142-158.

[6] Federico, I., Marrone, S., Colagrossi, A., Aristodemo, F., & Veltri, P. (2010). Simulation of hydraulic jump through sph model. *IDRA XXXII Italian Conference of Hydraulics and Hydraulic Construction.* Palermo, Italy.

[7] Lucy, L. B. (1977). A numerical approach to testing of the fission hypothesis. *The Astronomical Journal*, 1013-1024.

[8] Gingold, R. A., & Monaghan, J. J. (1977). Smoothed particle hydrodynamics: theory and application to non-spherical stars. *Monthly Notices of the Poyal Astronomical Society, 181*, 375-389.

[9] Liu, G. R., & Liu, M. B. (2009). *Smoothed Particle Hydrodynamics : a meshfree particle method.* Singapore: World Publishing Co. Pte. Ltd.

[10] Quinlan, N. J., Basa, M., & Lastiwka, M. (2006). Truncation error in mesh-free methods. *International Journal for Numerical Methos in Engineering*, 66:2064-2085.

[11] Graham, D. I., & Hughes, J. P. (2008). Accuracy of SPH viscous flow models. *International Journal for Numerical Methods in Fluids*, 56:1261-1269.
[12] Vesenjak, M., Müllerschön, H., Hummel, A., & Ren, Z. (2004). Simulation of Fuel Sloshing - Comperative Study. *LS-DYNA Anwenderforum*. Bamberg: DYNAmore GmgH.
[13] Varas, D., Zaera, R., & López-Puente, J. (2009). Numerical modeling of hydrodynamic ram phenomenon. *International Journal of impact Engineering 36*, 363-374.
[14] LSTC. (2010). *LS-DYNA Keyword User´s Manual Version 971 Rev 5*. Livermore: Livermore Software Technology Corporation (LSTC).
[15] Hallquist, J. O. (2006). *LS-DYNA Theory Manual*. Livermore Software Technology Corporation.
[16] Lennon, J. M., & Hill, D. F. (2006). Particle Image Velocity Measurements of Undular and Hydraulic Jumps. *Journal of Hydraulic Engineering*, 1283-1294.